Cosmic Axion Background Detection Using Resonant Cavity Arrays

Soobeom (Leo) Chung

May 12, 2026

arXiv:2508.03797

University of Florida

Outline

- Cosmic Axion Background (CaB)
- ADMX
- Correlation function
- Sensitivity of resonant cavity arrays

Cosmic Axion Background

- Peccei-Quinn Mechanism (1977) to resolve the strong CP problem in QCD
- Axions can have important implications for astrophysics and cosmology.
  - Contribute to radiative energy loss of a star
  - Dark matter
- **Relativistic axions** could have been produced in the early universe that may effect the expansion history (Dror, 2021)

Cosmic Axion Background

- Thermal relic
  - Axions in thermal contact with SM at high temperature can generate background like CMB
- Dark matter decay
  - galactic DM within the Milky Way and extragalactic DM throughout the universe

Detecting CaB

- The CaB behaves as an oscillating classical wave
- Unlike non-relativistic axion $(\Delta\omega/\omega \sim 10^{-6})$, the C$a$B has a broad energy spectrum and shorter coherence length/time $(\Delta\omega/\omega \sim 1)$
  - $\omega \simeq m_a(1 + \frac{v^2}{2})$ for non-relativistic axion
- ADMX is the closest to being sensitive to cosmological relics.

ADMX

- Axion haloscope with a resonant cavity with typical target scale ($\omega_0 = j_{10}/R$): $\sim \mu\text{eV}$ (ADMX, 2018)
- Inverse Primakoff interaction (Sikivie, 1984):

$$\mathcal{L} \supset g_{a\gamma\gamma}\, a\, \mathbf{E} \cdot \mathbf{B}$$

- $$\nabla \cdot \mathbf{E} = \rho - g_{a\gamma\gamma}\, \mathbf{B} \cdot \nabla a,$$
  $$\nabla \cdot \mathbf{B} = 0,$$
  $$\nabla \times \mathbf{E} = -\partial_t \mathbf{B},$$
  $$\nabla \times \mathbf{B} = \partial_t \mathbf{E} + \mathbf{J} + g_{a\gamma\gamma}(\mathbf{B}\, \partial_t a - \mathbf{E} \times \nabla a).$$

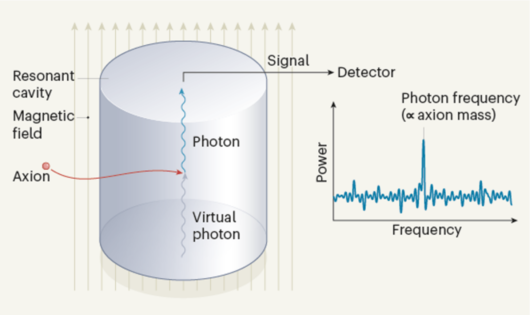

Computing the Correlation Function

- The real and imaginary part of the electric field correlation function for i-th and j-th cavity:

$$\left\langle \tilde{R}^{(i)} \tilde{R}^{*(j)} \right\rangle = \left\langle \tilde{I}^{(i)} \tilde{I}^{*(j)} \right\rangle = \left[\frac{4T_s^{(i)}}{Q\,\omega_0}\,\delta_{ij} + \frac{\pi\,(g_{a\gamma\gamma}B_0)^2\,V\omega_0}{2(2\pi)^3}\,f(\omega_0)\,\mathcal{F}_{ij} \right] |T(\omega)|^2.$$

Q : quality factor, $T_s^{(i)}$: temperature of i-th cavity, V: volume, $f(\omega)$: energy distribution

- Relativistic form factor

$$\mathcal{F}_{ij} = \frac{1}{V} \int d\hat{\mathbf{n}}\,\cos(\omega_0 \hat{\mathbf{n}} \cdot \mathbf{x}_0) \left| \int d^3x_i\, e^{i\omega_0 \hat{\mathbf{n}} \cdot \mathbf{x}_i}\, \hat{\mathbf{z}} \cdot \mathbf{e}^*(\mathbf{x}_i) \right|^2$$

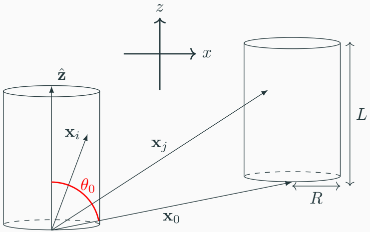

Self-correlation

$$\mathcal{F}_{11} \to \begin{cases} \dfrac{16\pi(1+2\mathcal{J})}{3j_{10}^2}, & \lambda \ll 1, \\ \dfrac{16\pi\mathcal{J}}{\lambda j_{10}^2}, & \lambda \gg 1, \end{cases}$$

$$\mathcal{J} \equiv \left[\frac{J_1(j_{10})j_{10}}{2}\right]^2, \lambda \equiv \omega_0 L$$

- Self-correlation falls as the cavity becomes longer
- Multiple oscillation cycles across the cavity suppress the response

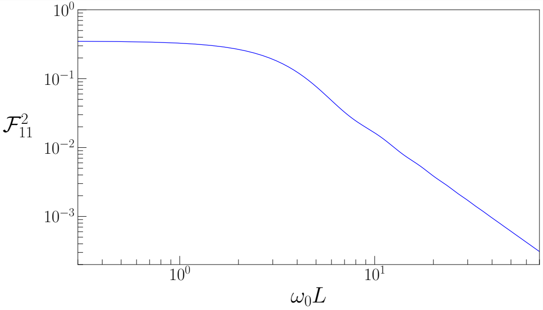

Coplanar array (blue) vs. vertical array (green)

- Much of the coplanar region is unphysical because of overlap constraints
- Vertical arrays can have larger usable correlation
- Current and future ADMX-like arrays are not optimal for CaB detection

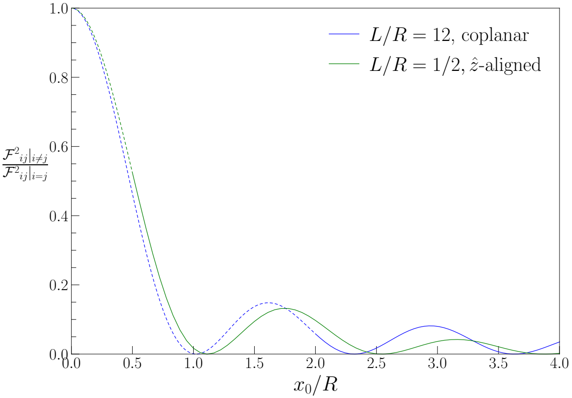

Sensitivity of Resonant Cavity Arrays

- Assuming an isotropic power-law axion relic energy density $\Omega_a(\omega) = \Omega_0 \left(\frac{\omega}{\omega_*}\right)^{\beta}$,

$$\Omega_0 \simeq 1.1 \times 10^{-3} \left(\frac{7\,\mathrm{T}}{B_0}\right)^2 \left(\frac{g_{a\gamma\gamma}^{\mathrm{SE}}}{g_{a\gamma\gamma}}\right)^2 \left(\frac{10^5}{Q}\right) \left(\frac{T_s}{148\,\mathrm{mK}}\right) \sqrt{\frac{100\,\mathrm{s}}{T}} \left(\frac{97\,\mathrm{cm}}{L}\right) \sqrt{\frac{4}{N}} \sqrt{\frac{1}{\bar{I}}}$$

$g_{a\gamma\gamma}^{\mathrm{SE}} = 6.6 \times 10^{-11}$GeV^{-1} (CAST 2017, Carenza 2020)

- Geometry and cavity number enter through the final brackets

$$\bar{I} \equiv \frac{1}{N} \sum_{ij} \int_{\omega_{\min}}^{\omega_{\max}} \frac{d\omega_0}{\omega_*} \left(\frac{\omega_0}{\omega_*}\right)^{2\beta-8} \mathcal{F}_{ij}^2$$

Sensitivity of Existing Proposals

- **ADMX run-2A** (Yang, 2020)
  - four-cavity array
  - $L = 97\,\mathrm{cm},\ R = 8\,\mathrm{cm}$
- **ADMX EFR** (Knirck, 2023)
  - 18-cavity array
  - $L = 97\,\mathrm{cm},\ R = 6.4\,\mathrm{cm}$
- For $\Delta N_{\mathrm{eff}} = 0.34$ (Planck 2018),

$$\Omega_0 \simeq 7 \times 10^{-6}$$

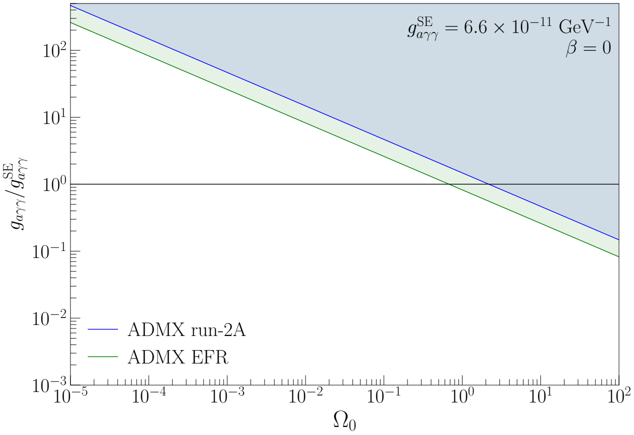

Optimizing the Parameters of the Array

- **Cavity height L**
- **Number of cavities scaling**
- Vertically stacked ‘fat’ arrays are favored

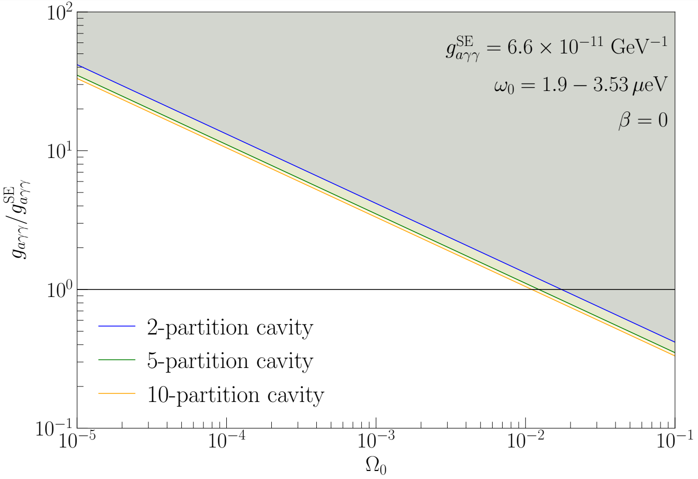

Conclusion

- Developed a CaB detection strategy using resonant cavity arrays motivated by ADMX
- Explored geometries and configurations that enhance signal correlations
- Further improvements:
    - extension to LC resonators and related platforms
        - long-lived, phase-coherent signals without being forced into cavity aspect ratio or packing geometry

Appendix

Self correlation

$$\mathcal{F}_{ii} = \frac{32\pi}{j_{01}^2\lambda^3}\left[\lambda - 2\mathcal{J}\lambda + \mathcal{J}\lambda\cos\lambda + (\mathcal{J}-1)\sin\lambda + \mathcal{J}\lambda^2\,\mathrm{Si}(\lambda)\right],$$

Fat cavity

$$\mathcal{F}_{ij} = \frac{8\pi}{j_{01}^2\chi^3}\left[(\mathcal{J}-1)\Big(\sin\chi - (1+3c_{2\theta_0})\chi\cos\chi - c_{2\theta_0}\sin\chi(\chi^2-3)\Big) + (\mathcal{J}+1)\chi^2\sin\chi\right],$$

Vertically separated

$$\mathcal{F}_{ij} = \frac{16\pi}{j_{01}^2\chi(\chi-\lambda)\lambda^2(\chi+\lambda)}\Big[2\chi\cos\lambda\Big(\mathcal{J}(\chi^2-\lambda^2)\cos\lambda + (\mathcal{J}-1)\chi\sin\chi\Big) - 2(\mathcal{J}-1)\chi\lambda\cos\chi\sin\lambda$$
$$+(\chi^2-\lambda^2)\Big(2\sin\chi - \frac{2\mathcal{J}}{\chi}(\chi\cos\chi+\sin\chi) + \mathcal{J}\chi\big(-2\chi\,\mathrm{Si}(\chi) + (\chi-\lambda)\,\mathrm{Si}(\chi-\lambda) + (\chi+\lambda)\,\mathrm{Si}(\chi+\lambda)\big)\Big)\Big]$$

Coplanar cavities

$$\mathcal{F}_{ij} = \frac{16\pi}{j_{01}^2}\sum_{\ell=0}^{\infty}\frac{(-1)^\ell 2^{\ell+\frac{1}{2}}\lambda^{2\ell}}{\chi^{\ell+\frac{3}{2}}}\left[(1+2\mathcal{J}+2\ell)J_{\ell+\frac{3}{2}}(\chi) - \mathcal{J}\chi J_{\ell+\frac{5}{2}}(\chi)\right]\frac{\Gamma\left(\ell+\frac{1}{2}\right)}{\Gamma(2\ell+3)}$$

Definitions

$$\lambda = \omega_0 L,\ \mathrm{Si}(x) \equiv \int_0^x \frac{\sin t}{t}\,dt,\ \mathcal{J} \equiv \left[\frac{J_1(j_{01})\,j_{01}}{2}\right]^2,\ \chi = \omega_0 x_0$$

Reference

- R. Peccei and H. R. Quinn, CP Conservation in the Presence of Instantons, Phys. Rev. Lett. 38 (1977) 1440–1443.
- R. Peccei and H. R. Quinn, Constraints Imposed by CP Conservation in the Presence of Instantons, Phys. Rev. D 16 (1977) 1791–1797.
- J.A. Dror, H. Murayama and N.L. Rodd, Cosmic axion background, Phys. Rev. D 103 (2021) 115004 [2101.09287]
- P. Sikivie, Experimental Tests of the Invisible Axion, Phys. Rev. Lett. 51 (1983) 1415–1417. [Erratum: Phys.Rev.Lett. 52, 695 (1984)].
- J. Yang, J.R. Gleason, S. Jois, I. Stern, P. Sikivie, N.S. Sullivan et al., Search for 5–9 eV, Axions with ADMX Four-Cavity Array, Springer Proc. Phys. 245 (2020) 53
- S. Knirck and A.C. Team, ADMX Extended Frequency Range (EFR): Searching for 2-4GHz axions with 18 cavities, in APS April Meeting Abstracts. vol. 2023 (2023) of APS Meeting Abstracts p. CCC01.002. 2023.
- ADMX collaboration, A Search for Invisible Axion Dark Matter with the Axion Dark Matter Experiment, Phys. Rev. Lett. 120 (2018) 151301 [1804.05750].
- ADMX collaboration, Extended Search for the Invisible Axion with the Axion Dark Matter Experiment, Phys. Rev. Lett. 124 (2020) 101303 [1910.08638].
- CAST collaboration, New CAST Limit on the Axion-Photon Interaction, Nature Phys. 13 (2017) 584 [1705.02290].
- P. Carenza, O. Straniero, B. D¨obrich, M. Giannotti, G. Lucente and A. Mirizzi, Constraints on the coupling with photons of heavy axion-like-particles from Globular Clusters, Phys. Lett. B 809 (2020) 135709 [2004.08399].